Procedia Computer Science

Volume 51, 2015, Pages 1229–1238

ICCS 2015 International Conference On Computational Science

An algorithm for the numerical solution of the pseudo compressible Navier-Stokes equations based on the experimenting fields approach

Amgad Salama*, Shuyu Sun, Mohamed F. El Amin

Computational Transport Phenomena Laboratory (CTPL), Division of Physical Sciences and Engineering (PSE), King Abdullah University of Science and Technology (KAUST), Thuwal 23955-6900, KSA.
Email: amgad.salama@kaust.edu.sa

Abstract
In this work, the experimenting fields approach is applied to the numerical solution of the Navier-Stokes equation for incompressible viscous flow. In this work, the solution is sought for both the pressure and velocity fields in the same time. Apparently, the correct velocity and pressure fields satisfy the governing equations and the boundary conditions. In this technique a set of predefined fields are introduced to the governing equations and the residues are calculated. The flow according to these fields will not satisfy the governing equations and the boundary conditions. However, the residues are used to construct the matrix of coefficients. Although, in this setup it seems trivial constructing the global matrix of coefficients, in other setups it can be quite involved. This technique separates the solver routine from the physics routines and therefore makes easy the coding and debugging procedures. We compare with few examples that demonstrate the capability of this technique.

Keywords: Navier-Stokes equations, the continuum hypothesis, numerical methods, experimenting field approach.

1 Introduction

The fascinating patterns of fluid motion at the macroscopic scale hinder different reality at the microscopic scale characterised by complete randomness and chaoticity. It also reveals that these orderly macroscopic motions may be described by a set of laws that are, in principle, physically consistent. This point of view conforms to our perception of fluids as continua in which the medium is continuous to any level of spatial resolution one might hope to reach. Apart from the fact that the concept of continuum is a mathematical abstraction to idealize the treatment of phenomena that are otherwise complex, it was able to provide us with sufficient tools that successfully describe many of the underlying macroscopic fluids fascination. In this sense, macroscopic field variables are

Selection and peer-review under responsibility of the Scientific Programme Committee of ICCS 2015

doi:10.1016/j.procs.2015.05.303

continuous functions of space and time and make readily available the arsenal of mathematical tools related to theories of continuous functions. A number of consequences, however, appear as a result of adapting the continuum hypothesis. The first is that new variables at the macroscopic description emerge that does not have counterparts at the microscopic scale (e.g., pressure, temperature, density, etc.). Even variables which have counterparts (e.g., velocity, acceleration, etc.) are now having different meanings. That is while the velocity at the microscopic scale is associated with a definite particle, it is at the macroscopic scale not associated with particles; rather it represents an average over representative volume of the velocity of the many particles contained within this volume. The averaging process generates, in addition to the averaged quantities, other quantities which are related to micro-scale variables and this makes the governing equations unclosed. This necessitates that two different mechanisms be hypothesized for the transport of conservative quantities, Leal [1]. The first is associated with the continuum motion and the second is related to the microscopic random motion of fluid particles projected over the continuum variables. For the transport of energy or solute the later mechanism describes what is known as the diffusion process and for momentum, it is more complicated, and generally describes surface stresses. Surface stresses are related to the transport of momentum by random motion of the particles across the direction of the bulk motion of the continuum. The notion of stress vector (force exerted on area) is introduced by Cauchy who hypothesized that this stress vector changes with the change of orientation of the areal element. That is stress vectors depend, in addition to the position and the time, on the orientation of the surface and is therefore a tensor quantity. Since these quantities depends on molecular exchange across area, it is important to relate them to macroscopic variables through constitutive relationships. Such constitutive relationships relate the net microscopic fluxes to the gradient of macroscopic variables through parameters that are dependent on the fluid (e.g., thermal conductivity, solute diffusion coefficient, viscosity, etc.). The governing equations describing conservation laws in isothermal fluid continua are those related to the conservation of mass and momentum. The derivation of such laws necessitates introducing the concept of control volume which is a mathematical abstraction employed in order to facilitate the derivation of the governing laws, Fig. 1. It is a volume fixed in space or moving with definite velocity through which fluid flows. The surface enclosing the control volume is referred to as the control surface. For a given control volume, the conservation equations may be presented as

- Mass conservation

$$\frac{\partial}{\partial t}\int_{\Omega}\rho d\Omega + \int_{S}\rho\mathbf{v}\cdot\mathbf{n}dS = 0 \qquad (1)$$

where ρ is the density, $\mathbf{v}$ is the velocity vector and $\mathbf{n}$ is the unit outward normal vector. Upon using the divergence theorem the above equation reduces to

$$\frac{\partial\rho}{\partial t} + \nabla\cdot\rho\mathbf{v} = 0 \qquad (2)$$

- Momentum conservation

$$\frac{\partial}{\partial t}\int_{\Omega}\rho\mathbf{v}d\Omega + \int_{S}\rho\mathbf{v}\mathbf{v}\cdot\mathbf{n}dS = \sum\mathbf{f} \qquad (3)$$

The right hand side considers all the external forces. This includes surface forces due to pressure, normal and shear viscous stresses, etc., and body forces which act on each point of the continuum within the control volume (gravity, Coriolis forces, etc.), Fig. 1. The above equation may be written as

$$\frac{\partial}{\partial t}\int_{\Omega}\rho\mathbf{v}d\Omega + \int_{S}\rho\mathbf{v}\mathbf{v}\cdot\mathbf{n}dS = \int_{S}\mathbf{T}\cdot\mathbf{n}dS + \int_{\Omega}\rho\mathbf{b}d\Omega \qquad (4)$$

where $\mathbf{T}$ is the stress vector. And again using the divergence theorem, the above equation reduces to

$$\frac{\partial \rho \mathbf{v}}{\partial t} + \nabla \cdot \rho \mathbf{v}\mathbf{v} = \nabla \cdot \mathbf{T} + \rho \mathbf{b} \tag{5}$$

The stress tensor, **T** in the above equation is defined as

$$\mathbf{T} = -\left[p - \left(\mu^v - \frac{2}{3}\mu\right)\nabla \cdot \mathbf{v}\right]\mathbf{I} + 2\mu\mathbf{D} \tag{6}$$

$$\mathbf{D} = \frac{1}{2}[\nabla \mathbf{v} + \nabla \mathbf{v}^T] \tag{7}$$

The viscous part of the stress tensor may be written as

$$\boldsymbol{\tau} = 2\mu\mathbf{D} + \left[\left(\mu^v - \frac{2}{3}\mu\right)\nabla \cdot \mathbf{v}\right]\mathbf{I} \tag{8}$$

$$\frac{\partial \rho \mathbf{v}}{\partial t} + \nabla \cdot \rho \mathbf{v}\mathbf{v} = -\nabla p + \nabla \cdot \boldsymbol{\tau} + \rho \mathbf{b} \tag{9}$$

$$\frac{\partial \rho \mathbf{v}}{\partial t} + \boldsymbol{\nabla} \cdot \rho \mathbf{v}\mathbf{v} = -\boldsymbol{\nabla} p + \boldsymbol{\nabla} \cdot \mu \nabla \mathbf{v} + \rho \mathbf{b} \tag{10}$$

The solution of this set of equations is obtained, usually, numerically for which there exist a number of schemes as will be explained in the next section.

2 On the numerical solution of the Navier-Stokes equations

The above mentioned set of equations describes both laminar and turbulent flow scenarios. However, when the flow is turbulent, the numerical solution of these equations requires a very dense mesh to resolve all the length and time scales typically associated with turbulent flow regimes which pose real challenges when modelling real flow problems. The difficulties associated with the numerical solution of the governing equations stems from the highly non-linear features of the Navier-Stokes equations when the flow conditions are turbulent. There is a great deal of motivation, therefore, to simplify the governing equations by time averaging and model the obtained turbulence stresses. The numerical solution of the NS equations is sometimes refers to as computational fluid dynamics, CFD, which has been the subject of intensive research. The number of literatures available that covers all aspects and techniques are enormous to be presented in this work. Several textbooks are available which cover a wide range of methods and algorithms including the finite differences method, the finite elements methods and their variants, finite volumes method and others [2-6]. The numerical solution of the governing equations involve spatial and temporal (in case of time-dependent problems) discretization. The simplest explicit forward step for incompressible NS equations may take the form

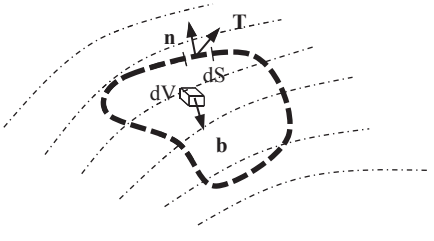

Fig. 1 Schematic of a typical control volume.

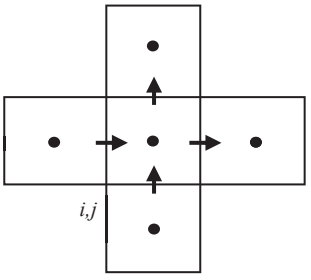

Fig. 2 Typical finite volume staggered grid

$$v^{k+1} = v^k + \Delta t\left(-v^k \cdot \nabla v^k - \frac{1}{\rho}\nabla p^k + \upsilon \nabla^2 v^k + g^k\right) \tag{11}$$

where Δt is the time step and the superscript k denotes the previous time step. However, the velocity calculated based on this approach does not, generally, satisfy the continuity. In other words $\nabla \cdot \mathbf{v}^{k+1} \neq 0$ and also there is no natural computation for p^{k+1}. One remedy to this difficulty is to take the pressure at the new time step such that

$$v^{k+1} + \frac{\Delta t}{\rho}\nabla p^{k+1} = v^k + \Delta t(-v^k \cdot \nabla v^k + \upsilon \nabla^2 v^k + g^k) \tag{12}$$

$$\nabla \cdot v^{k+1} = 0 \tag{13}$$

Now, by taking the divergence of Eq. 16, one obtains a Poisson-like equation for the pressure

$$\nabla^2 p^{k+1} = \frac{\rho}{\Delta t}\nabla \cdot (v^k - \Delta t v^k \cdot \nabla v^k + \Delta t \upsilon \nabla^2 v^k + \Delta t g^k) \tag{14}$$

A semi-implicit scheme can also be developed such that

$$(1 + \Delta t v^k \cdot \nabla - \Delta t \upsilon \nabla^2) v^{k+1} + \frac{\Delta t}{\rho}\nabla p^{k+1} = v^k \tag{15}$$

$$\nabla \cdot v^{k+1} = 0$$

The solution of this system requires a pair of compatible pressure and velocity spaces to solve the system resulting in the discrete system to be coupled. In other words, a global linear system may be constructed of the form

$$\begin{bmatrix} A & B \\ B^T & 0 \end{bmatrix}\begin{bmatrix} \mathbf{v} \\ \mathbf{p} \end{bmatrix} = \begin{bmatrix} \mathbf{f} \\ 0 \end{bmatrix} \tag{16}$$

where the vector **v** contains all the velocity components and $\boldsymbol{p}$ is the pressure vector. Mixed finite element (MFE) is an example of the methods which works with different basis functions for both the velocity and the pressure. In the realm of NS algorithms using MFE, it is customary to use quadratic piece-wise polynomials for the velocity and linear piecewise polynomial for the pressure. MFE applied to the numerical solution of the NS produces a linear system as given in (16). Moreover, finite difference schemes working on staggered grid, Fig. 2, can also lead to similar system as given in (16). As outlined in Langtangen et al. [7], this system, in some cases, can be singular and requires special discretization or stabilizing techniques to ensure invertible matrix. The singularity of such system can be circumvented by introducing a stabilization matrix, $\varepsilon \boldsymbol{D}$, and a perturbation of the right hand side, $\varepsilon \boldsymbol{d}$, Langtangen et al. [7] such that the global system is

$$\begin{bmatrix} A & B \\ B^T & -\varepsilon D \end{bmatrix}\begin{bmatrix} v \\ p \end{bmatrix} = \begin{bmatrix} f \\ -\varepsilon d \end{bmatrix} \tag{17}$$

The parameter ε is usually taken as constant, however, for some more involved problems including anisotropic mesh, it can be local (i.e., dependent on the location). Such stabilizing matrices are constructed based on some heuristic approaches or by some physical assumptions. They are all based on adding a pressure term to the continuity equation. A number of such possibilities include

$$\nabla \cdot \mathbf{v} + \varepsilon p = 0 \qquad \text{in } \Omega \tag{18}$$

$$\nabla \cdot \mathbf{v} + \varepsilon \frac{\partial p}{\partial t} = 0 \qquad \text{in } \Omega \tag{19}$$

$$\nabla \cdot \mathbf{v} - \varepsilon \Delta p = 0 \qquad \text{in } \Omega\,, \frac{\partial p}{\partial n}\Big|_{\partial\Omega} = 0 \tag{20}$$

$$\nabla \cdot \mathbf{v} - \varepsilon \Delta \frac{\partial p}{\partial t} = 0 \qquad \text{in } \Omega, \frac{\partial p_{,t}}{\partial n}\Big|_{\partial\Omega} = 0 \tag{21}$$

Eq. 19 above has some relevance to the problem of flow of compressible fluids. For compressible flow, the NS equations take the form:

$$\rho\left(\frac{\partial \mathbf{v}}{\partial t} + \mathbf{v} \cdot \nabla \mathbf{v}\right) = -\nabla p + \nabla \cdot \mu(\nabla \mathbf{v} + \nabla \mathbf{v}^T) + \nabla(\lambda \nabla \cdot \mathbf{v}) + \rho \mathbf{g} \tag{22}$$

$$\frac{\partial \rho}{\partial t} + \nabla \cdot \rho \mathbf{v} = 0 \tag{23}$$

where λ is the second coefficient of viscosity (bulk viscosity). If we consider fluid with little compressibility, then it may be possible to neglect the bulk viscosity. Under such condition, a linearized equation of state for isothermal fluid relates the pressure and density such that:

$$p = p(\rho) \approx p_0 + c_0^2(\rho - \rho_0) \tag{24}$$

With $c_0^2 = \partial p \,/\, \partial \rho|_{(p_0,\rho_0)}$ is the speed of sound. Eq. 23 therefore may be written as

$$\frac{\partial p}{\partial t} + c_0^2 \rho_0 \nabla \cdot \mathbf{v} = 0 \tag{25}$$

Let $1/\varepsilon = c_0^2 \rho_0$, and manipulating the above equation one obtains Eq. 19. The application of the pseudo-compressibility transient term converts the elliptic system of incompressible flow equations into a set of hyperbolic type equations. Ideally the value of the pseudo compressibility is to be chosen such that the speed of propagation of disturbances approaches that of the incompressible flow. On the other hand if the pseudo-compressibility parameter is chosen such that the speed of disturbance propagation is too slow, the variation of the pressure field accompanying these waves will, likewise, be slow.

3 The experimenting field approach

The numerical solution of this equation is based on the experimenting fields approach. In this approach a set of experimenting fields are applied to the governing equations as will be detailed later in this section. This technique has been developed and applied to several transport phenomena in porous media and show to be efficient and robust [8-14]. In this work we extend it to a more general framework. The governing equations based on pseudo compressibility may be written as:

$$\varepsilon \frac{\partial p}{\partial t} + \nabla \cdot \mathbf{v} = 0 \tag{26}$$

$$\frac{\partial \mathbf{v}}{\partial t} + (\mathbf{v} \cdot \nabla)\mathbf{v} = -\frac{1}{\rho}\nabla p + \upsilon \nabla^2 \mathbf{v} \tag{27}$$

Using semi-implicit numerical technique, the above equations may be written as

$$\frac{v^{k+1} - v^k}{\Delta t} + (v^k \cdot \nabla)v^{k+1} = -\frac{1}{\rho}\nabla p^{k+1} + \upsilon \nabla^2 v^{k+1} \tag{28}$$

$$(1 + \Delta t v^k \cdot \nabla - \Delta t \upsilon \nabla^2)v^{k+1} + \frac{\Delta t}{\rho}\nabla p^{k+1} = v^k \tag{29}$$

$$\varepsilon \frac{p^{k+1}-p^k}{\Delta t} + \nabla \cdot v^{k+1} = 0 \tag{30}$$

$$\nabla \cdot v^{k+1} + \frac{\varepsilon}{\Delta t} p^{k+1} = \frac{\varepsilon}{\Delta t} p^k \tag{31}$$

With some discretization in space, a linear system may be constructed. For this purpose and without loss of generality, we consider the cell-centered finite differences approximation of the governing equations. We define a simple 2D problem in a rectangular domain, Ω: $(a_1,b_1)\times(a_2,b_2)$, filled with a single fluid. The approximation is thought over the rectangular mesh defined by $\{x_0, x_1, x_2, \cdots x_i, \cdots, x_m\} \times \{y_0, y_1, y_2, \cdots, y_j, \cdots, y_n\}$, where *m*, *n* are the number of segments in *x* and *y* directions, respectively. Using staggered grid settings (Fig.2), the velocity is defined at the edges and the pressure at the center of the cells. The discretized equations can be written in matrix form as

$$A_{xx}u + A_{xp}p = f_u \tag{32}$$

$$A_{yy}v + A_{yp}p = f_y \tag{33}$$

$$A_{cx}u + A_{cy}v - A_{cp}p = d \tag{34}$$

The global linear system, therefore, may be written as:

$$\begin{bmatrix} A_{xx} & A_{xy} & A_{xp} \\ A_{xy}^T & A_{yy} & A_{yp} \\ A_{cx} & A_{cy} & A_{cp} \end{bmatrix} \begin{bmatrix} u \\ v \\ p \end{bmatrix} = \begin{bmatrix} f_x \\ f_y \\ d \end{bmatrix} \tag{35}$$

where $A_{xx}: (m+1)n \times (m+1)n$, $A_{xy}: (m+1)n \times (n+1)m$, $A_{xp}: (m+1)n \times nm$ $A_{yy}: (n+1)m \times (n+1)m$, $A_{yp}: (n+1)m \times nm$, $A_{cx}: mn \times (m+1)n$, $A_{cy}: mn \times (n+1)m$ and $A_{cp}: mn \times mn$. In this system, the right hand side includes contribution of the boundary conditions and the source/sink term such that

$$f_x = f^u + f_x^p \tag{36}$$

$$f_y = f^v + f_y^p \tag{37}$$

$$d = d_u + d_v + d_p \tag{38}$$

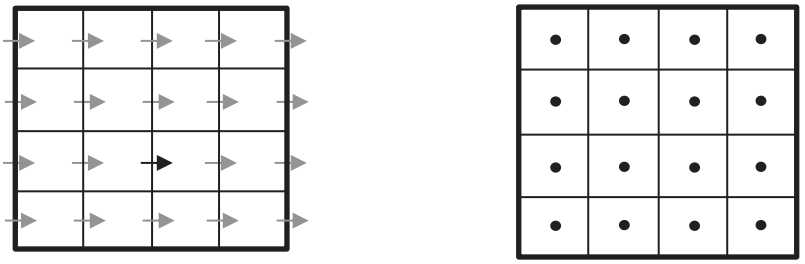

(a) (b)

Fig. 3 Experimenting fields (a) *x*-velocity field and (b) pressure field

In the experimenting fields approach, the matrix of coefficients is constructed automatically by

experimenting on the system with $(m+1)n+(n+1)m+mn$ predefined fields. The block matrices at the diagonal, as an example, are the discretized version of the differential operators as suggested by Eqs. 29 and 31. For example, we have

$$(1+\Delta t u^k\cdot\nabla-\Delta t v\nabla^2)\overset{\Delta}{\rightarrow}A_{xx},A_{yy} \tag{39}$$

$$\varepsilon\frac{\partial}{\partial t}\overset{\Delta}{\rightarrow}A_{cp} \tag{40}$$

Such that

$$A_{xx}u=\sum_{j=1}^{(m+1)n}a_{ij}^{u}\,u_j=f^{u}=c_i u_i^{B} \tag{41}$$

$$A_{yy}v=\sum_{j=1}^{m(n+1)}a_{ij}^{v}\,v_j=f^{v}=c_i v_i^{B} \tag{42}$$

$$A_{cp}p=\sum_{j=1}^{mn}a_{ij}^{p}\,p_j=d_p=c_i p_i^{B} \tag{43}$$

Apparently, if the velocity and pressure fields are the correct fields satisfying the governing equations and the boundary condition, the global system satisfy the equality as given in Eq. 22. If, however, the velocity and pressure fields are not the correct fields, Eq. 22 is not satisfied. Moreover, since the system is linear, a correct subfield (i.e., *u*, *v* or *p*) would satisfy their own system but not the global one. In other words, if *u* is the correct velocity field in the *x*-direction, Eq. 28 is satisfied but not the global system given in Eq. 22. We use this property to examine the behavior of the different systems to specific kinds of fields and how the different matrices composing the global system are constructed. As an example, consider how the matrix A_{xx} is evaluated. The system given by Eq. 41 may be written as:

$$\begin{bmatrix} a_{1,1} & a_{1,2} & \cdots & \cdots & a_{1,m} & \cdots & \cdots & \cdots \\ a_{2,1} & a_{2,2} & a_{2,3} & \cdots & \cdots & a_{2,(m+1)} & \cdots & \vdots \\ \vdots & \cdots & \cdots & \cdots & \cdots & \cdots & \vdots & \vdots \\ \vdots & & & & & \vdots & \vdots & \vdots \\ \vdots & & & & & \vdots & \vdots & \vdots \\ \vdots & \cdots & \cdots & \cdots & \cdots & \vdots & \vdots & a_{(m+1)n,(m+1)n} \end{bmatrix}\begin{bmatrix} u_1 \\ u_2 \\ \vdots \\ \vdots \\ \vdots \\ u_{(m+1)n} \end{bmatrix}=\begin{bmatrix} f_1^{u} \\ f_2^{u} \\ \vdots \\ \vdots \\ \vdots \\ f_{(m+1)n}^{u} \end{bmatrix} \tag{44}$$

If the entries of the matrix A_{xx} are known, then, as mentioned earlier, the only *x*-velocity field that satisfies the equality is the correct field which satisfies the global system and the boundary conditions. Any other field will not satisfy the equality. However, consider applying a particular velocity field in the *x*-direction which is one at one location (i.e., at one edge) and zero elsewhere as shown in Fig.3-a. If this field is applied to system 44, the column of the matrix of coefficients corresponding to the location of the *x*-velocity which is one can be obtained. As shown in system 44, the first column is determined given this particular velocity field.

$$\begin{bmatrix} a_{1,1} & a_{1,2} & \cdots & \cdots & a_{1,m} & \cdots & \cdots & \cdots \\ a_{2,1} & a_{2,2} & a_{2,3} & \cdots & \cdots & a_{2,(m+1)} & \cdots & \vdots \\ \vdots & \cdots & \cdots & \cdots & \cdots & \cdots & \vdots & \vdots \\ \vdots & & & & & \vdots & \vdots & \vdots \\ \vdots & & & & & \vdots & \vdots & \vdots \\ \vdots & \cdots & \cdots & \cdots & \cdots & \vdots & \vdots & a_{(m+1)n,(m+1)n} \end{bmatrix}\begin{bmatrix} 1 \\ 0 \\ 0 \\ 0 \\ 0 \\ 0 \end{bmatrix}=\begin{bmatrix} res_1 \\ res_2 \\ \\ \\ \\ res_{(m+1)n} \end{bmatrix} \tag{45}$$

For this particular example

$$a_{1,1}=res_1$$

$$a_{2,1} = res_2,$$
$$\vdots$$
$$a_{(m+1)n,1} = res_{(m+1)n}$$

The residual is calculated by applying the experimenting field to the discretized equation of

$$(1 + \Delta t \mathbf{u}^k \cdot \nabla - \Delta t \upsilon \nabla^2)\boldsymbol{u}_{exp} \rightarrow \boldsymbol{res}$$

Figure 4 shows a schematic of the matrices constructing technique. This relationship implies that one needs to solve local problems for every single cell or edge which is apparently easier and at the background constructing the global matrix of coefficients and then solving the global system. There is, however, the disadvantage that one is required to solving large number of local problem in order to construct the matrix of coefficients. However, based on our understanding of the local stencil, it is possible to significantly reduce the number of local problems. For example, for first order approximation of the velocity and pressure derivatives, only nine times that such local problems may be solved if one takes the experimenting fields which do not overlap stencils of the local problems, Fig. 3-b. When the experimenting pressure field is all zeros, the residue calculates the contribution of the boundary conditions.

4 Numerical Examples: Lid driven cavity

In order to investigate the effect of the value of pseudo compressibility parameter on the steady state solution of the NS equations, a bench mark problem, namely the Lid driven flow problem, has been investigated. In this set up a square domain is considered filled with porous medium saturated with a single fluid. The domain boundaries are impermeable and the top boundary moves at a tangential speed u_0 as shown in Fig.5. The results are compared with the benchmark problem of Ghia [14] and very good match is obtained as shown in Figs. 6-9.

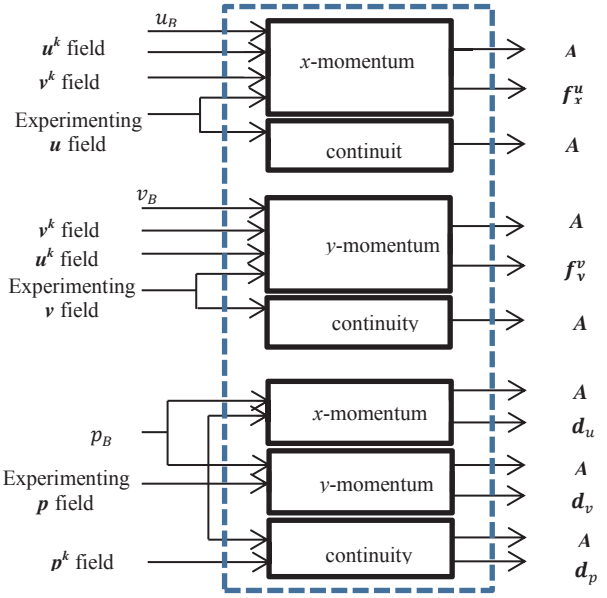

Fig. 4 Schematic chart for constructing different matrices and the right hand side

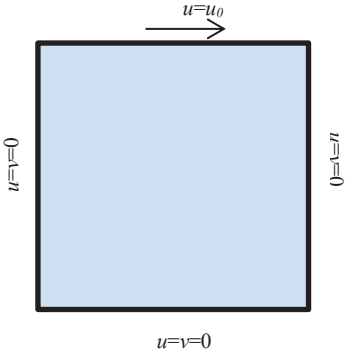

Fig.5 Schematic of the computational domain

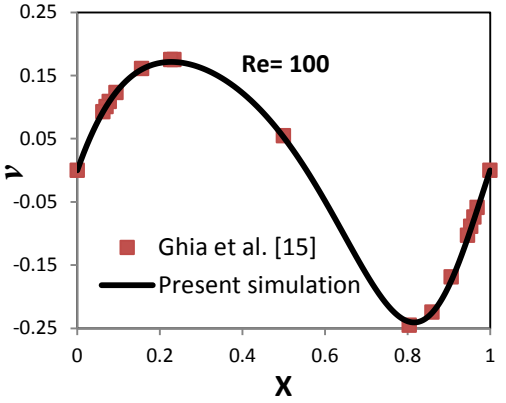

Fig. 6 Y-velocity component along the horizontal centreline (Re=100)

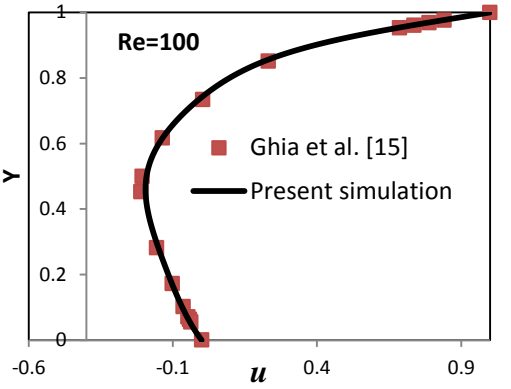

Fig. 7 X-velocity component along the vertical centreline (Re=100)

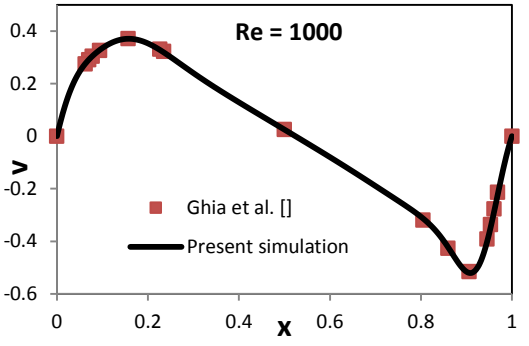

Fig. 8 Y-velocity component along the horizontal centreline (Re=1000)

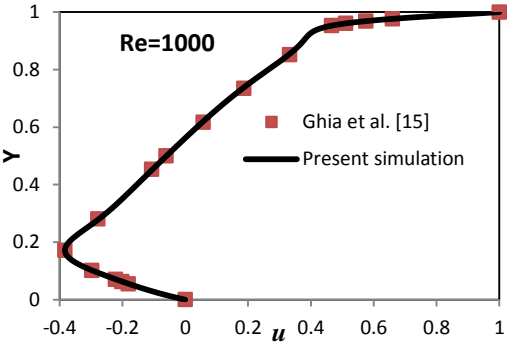

Fig. 9 X-velocity component along the vertical centreline (Re=1000)

5 Conclusion

In this work we introduce the use of the experimenting fields approach to the numerical solution of the Navier-Stokes equations. In this approach a number of predefined experimenting fields are operated on the discretized equations to construct automatically the global system. A number of local problems equal to the number of unknown variables are solved to generate such coefficients. However, such number of local problems can be significantly reduced to only 9 fields (in 2D) and therefore significantly reduce CPU time. We compare the results obtained by this technique and those found in literatures and very good match is obtained.

References

1. L.G. Leal, Advanced transport processes, Cambridge Series in Chemical Engineering, (2010)
2. J.H. Ferziger and M. Peric, Computational Methods for Fluid Dynamics, Springer Verlag, 2nd ed. (1999)
3. J.D. Anderson, Computational Fluid Dynamics: The Basics with Applications McGraw Hill, 6th ed, (1995)
4. O. Zikanov, Essential Computational Fluid Dynamics, Wiley, (2010)
5. J. Tu, G. H. Yeoh, C. Liu, Computational Fluid Dynamics: A Practical Approach, Butterworth-Heinemann; 2nd ed. (2012)
6. H. Versteeg, W. Malalasekera, An Introduction to Computational Fluid Dynamics: The Finite Volume Method, Prentice Hall; 2nd ed. (2007)
7. H.P. Langtangena, K-A. Mardala, R. Winther, Numerical methods for incompressible viscous flow, Advances in Water Resources 25, 8–12, (2002U, pp. 1125–1146.
8. A. Salama, S. Sun, M. Wheeler, Solving global problem by considering multitude of local problems: application to flow in anisotropic porous media using the multipoint flux approximation, J. Computational and Applied Mathematics, 267, (2014) PP. 117-130.
9. A. Salama, S. Sun, M.F. El Amin, Investigation of thermal energy transport from an anisotropic central heating element to the adjacent channels: A multipoint flux approximation, Annals of Nuclear Energy, 76, (2015) pp. 100-112.
10. A. Salama, W. Li, S. Sun, Finite volume approximation of the three- dimensional flow equation in axisymmetric, heterogeneous porous media based on local analytical solution, Journal of Hydrology, 501, (2013) 45–55.
11. A. Salama, S. Sun, M.F. El Amin, A multi-point flux approximation of the steady state heat conduction equation in anisotropic media, ASME J. Heat Transfer, 135, (2013) 1-6.
12. S. Sun, A., Salama, M.F. El Amin, An Equation-Type Approach for the Numerical Solution of the Partial Differential Equations Governing Transport Phenomena in Porous Media, Procedia Computer Science, 9, (2012), pp. 661-669
13. A. Negara, A. Salama, S. Sun, 3-D Numerical Investigation of Subsurface Flow in Anisotropic Porous Media using Multipoint Flux Approximation Method, Accepted for presentation in SPE Reservoir Characterization and Simulation Conference and Exhibition, Abu Dhabi, UAE, 16–18 September, SPE 165960, (2013)
14. A. Negara, A. Salama, S. Sun, Multiphase flow simulation with gravity effect in anisotropic porous media using multipoint flux approximation, Computers & Fluids, 114, 66-74 (2015)
15. G. Ghia, and Shin, "High-Re solutions for incompressible flow using the Navier-Stokes equations and a multigrid method", Journal of Computational Physics, 48, (1982) pp. 387-411.